

Mechanotransduction is the Janus-faced regulator of cell aging

Xiaojing Liu

West China Hospital of Stomatology, Sichuan University

Li Liao

West China Hospital of Stomatology, Sichuan University <https://orcid.org/0000-0003-0030-1009>

Peng Wang

sichuan university

Yuanxin Ye

sichuan university

Xiangyu Dong

sichuan university

Xiaotao Xing

sichuan university

Zhonghan Li

sichuan university

Qiang Wei (✉ wei@scu.edu.cn)

Sichuan University <https://orcid.org/0000-0001-5194-8262>

Weidong Tian

West China Hospital of Stomatology, Sichuan University

Article

Keywords:

Posted Date: November 8th, 2022

DOI: <https://doi.org/10.21203/rs.3.rs-2208259/v1>

License:   This work is licensed under a Creative Commons Attribution 4.0 International License.

[Read Full License](#)

Abstract

Aging is inevitable during development, and we still lack methods to rejuvenate it due to the poor understanding. A wealth of studies focused on the biochemical signaling pathways for inducing cell senescence, whereas the role of mechanotransduction during the process had been ignored. Here, we clarified how cell mechanosensing was involved and played functional roles in cellular senescence. The intracellular traction force and mechanotransduction could reduce in response to mesenchymal stem/stromal cell aging. Compensating the cell traction force via physical or chemical stimulation seems an attractive strategy for temporarily reversing aging markers, however, mechanical overstimulation triggers accelerated cellular senescence shortly afterwards. We further clarified that DNA damage results in the reduction of cellular mechanotransduction, which is a self-protective mechanism as it endows cells with resistance to further DNA damage, although it inhibits cell proliferation and many other functions. Taken together, we have disclosed the interplay between DNA damage, cellular mechanics, and senescence, confirming the two-side effects of the mechanical cues in the aging process.

Introduction

Age-related bone loss is a complicated event resulting from the decline in bone formation and the increase in bone resorption^{1,2}, accompanied by the deterioration of bone microstructure and the occurrence of several diseases like osteoarthritis, osteoporosis, and even bone fracture³⁻⁵. Numerous studies have found that with aging, multiple cell types including bone marrow mesenchymal stem/stromal cells (BMSCs) in the bone microenvironment become senescent and exhibit reduced osteogenic and self-renewal capacity, which would dampen bone remodeling, induce tissue dysfunction, and trigger skeleton aging⁶⁻⁸. Although delay or prevention of aging has recently gained momentum, discovering the mechanism to drive BMSC senescence is needed for finding effective strategies to ameliorate aging and these age-related skeleton diseases.

Although several hallmarks of aging act in concert to exacerbate the aging process, the generation of DNA damage plays a central role because it could precipitate the appearance of other aging-associated features at the molecular, cellular and physiological level⁹. Despite accumulating DNA damage is responsible for provoking cellular senescence¹⁰ and stem cell exhaustion¹¹, the mechanisms have not been fully elucidated. Thus, a deeper understanding of the underlying mechanism via which DNA damage induces cellular senescence is critical for developing more effective interventions to delay BMSC aging and overcome senescence barriers.

BMSCs reside in their own microenvironment, where they sense, react to, and convert countless biochemical as well as mechanical signals¹². Upon aging, alterations in stem cell mechanics¹³ and bone microenvironment where they dwell in have been observed¹⁴. Moreover, stem cells have the potential for adapting to the environment through mechanosensing¹⁵, so we hypothesized that cells might have variation in cellular mechanotransduction upon senescence. Although some studies have elaborated that

inhibition of cellular mechanotransduction pathways has many implications for cell behaviors¹⁶, like cell mechanics¹⁷, differentiation¹⁸, and migration¹⁹, relatively little is known about whether there is the engagement of the mechanotransduction in aging.

Recent research demonstrated that aged cells are accompanied by a universal decline in the openness of chromatin landscape, resulting in the alteration of transcriptional output and gene expression²⁰⁻²². Coincidentally some studies have revealed that microenvironments have effects on chromatin remodeling in human MSCs, leading to widespread changes in gene expression^{23,24}. Therefore, it is reasonable to hypothesize that chromatin accessibility might act as a bridge to connect mechanotransduction activity with cellular senescence. Understanding the interplay between DNA damage, mechanical characteristics and cellular senescence is quite vital and it might enable new approaches to intervene aging process.

In this study, we have revealed that cellular mechanotransduction diminishes with aging, but reacts to the regulation of senescence with two-side effects. It sheds light on the complex role of mechanical stimuli in the aging process.

Results

The cells in the bone tissue of aged mice lack mechanotransduction activity.

As shown in Fig. 1A-1C, the 20-month mice had significantly less trabecular numbers, greater trabecular spacing as well as lower levels of collagen I, comparing with 6-week mice. Deterioration in bone micro-architecture with age influenced the niche where BMSCs are located in, so it was worth investigating the mechanotransduction pathways of the cells in the tissue. The phosphorylation of focal adhesion kinase (p-FAK) at Tyr397²⁵ and the YAP expression²⁶ are well-known mechanotransduction markers and are sensitive to intracellular traction force. The immunohistochemistry results displayed that p-FAK, and YAP are significantly downregulated in the bone marrow-derived tissue from aged mice (20-month) compared with the tissue derived from young ones (6-week) (Fig. 1D,1E). The discrepancy in aging marker p16^{INK4a} and phosphorylation of the Ser139 residue of the histone variant H2AX (γ H2AX) between different ages were also obvious and old tissue had a higher degree of them than young tissue, indicating the senescence at the cellular level (Supplementary Fig. 1). These results revealed that bone marrow exists an age-related general decline in the activity of cellular mechanotransduction.

Cellular mechanotransduction decreases in senescent stem cells.

To understand the relationship between cell senescence and mechanotransduction in detail, human BMSCs were isolated and studied in vitro. The BMSCs from old (60 ~ 80 years old) and young (18 ~ 30 years old) donors were cultured and characterized by flow cytometry, proliferation assay, multilineage differentiation assays, and senescence-associated biomarkers (Supplementary Fig. 2) (Fig. 2A). The BMSCs from old patients exhibited impaired proliferative and osteogenic capacities as well as high

expressions of senescence-associated biomarkers compared to their counterparts isolated from young patients, suggesting that aging potentially changed the function of the stem cells. Thus, they were regarded as senescent and young cells, respectively, in the following experiments. In case of the variability between individual donors, we pooled cells obtained from three different donors together in each biological replicate.

To investigate the alteration of cellular mechanotransduction at the protein level, we performed immunofluorescence studies using a series of markers which are the essential factors in cellular mechanotransduction. The results revealed that senescent BMSCs from elderly patients have a global decline in total Myosin IIa (traction force generator), phosphorylated myosin IIa at Ser1943 (P-myosin IIa, activated Myosin IIa), Lamin A/C (nucleoskeleton that receives and transmits mechanic cue into the nucleus), as well as nucleus localization of YAP (transcriptional regulator that responding to mechanical cues), compared with cells from young donors, sharply contrasting with increased aging marker p16^{INK4a} during aging (Fig. 2A, 2B). Upon further western-blot assays, a significant reduction of these proteins was observed in senescent cells, and it was basically in line with the results of immunofluorescence (Fig. 2C). The alteration of the mechanotransduction factors affected cell mechanics and traction force. Nanoindentation showed that Young's modulus of aged cells was around 470 Pa and Young's modulus of young cells was about 790 Pa (Fig. 2D). According to the results of traction force microscopy, marked differences in traction force also existed between aged cells and young cells. The average force was about 122 Pa and 227 Pa, respectively (Fig. 2E, 2G). Moreover, the orientation and anisotropy of actin stress fibers, which mirrored intracellular traction force²⁷, was randomly distributed in the senescent cells but well aligned in the young cells (Fig. 2F, 2G). These data verified that there is a strong correlation between cellular senescence and the loss of mechanotransduction and mechanotransmission.

Finally, we considered whether the decreased cellular mechanotransduction is a common hallmark for BMSCs' aging in different species. To this end, the levels of Myosin IIa, P-myosin IIa, as well as Lamin A/C were examined in the bone marrow mesenchymal stromal cells (BMSCs) derived from mice (Supplementary Fig. 3). The results also exhibited similar changes as the human BMSCs, further validating our observation that senescent cells are accompanied by a deficiency in cellular mechanotransduction.

Cellular mechanotransduction regulates cell senescence.

We have verified that there are marked differences in mechanical characteristics between young and senescent cells. According to this, we hypothesized that the decline in cellular mechanotransduction could trigger young cell dysfunction and senescence. To mimic the depletion of mechanical stimuli, BMSCs were treated with blebbistatin, a myosin inhibitor mostly specific for myosin II that could efficiently erase the intracellular traction. The other effective model was soft hydrogels with a shear modulus of 1.5 kPa, which could modulate the force balance at the cell adhesive interface to decrease the intracellular traction force. After validating the success of the mechanotransduction depletion (Supplementary Fig. 4), the level of cyclin-dependent kinase inhibitors including p16^{INK4a}, p53, and p21

WAF1/Cip1 was examined, as they are well-known signs of cell senescence. Attenuation of cellular mechanotransduction, either through pharmacological or mechanical treatment, could induce age-related phenotypes and trigger stem cell senescence. (Fig. 3A and Supplementary Fig. 6A, 6C). The tendency was further validated through senescence-associated beta-galactosidase (SA- β -gal) staining (Fig. 3B), thereby proving that the decreased cellular mechanotransduction was the driver of senescence.

The decreased mechanotransduction of senescent cells was then restored by means of calyculin A, the myosin light chain phosphatase inhibitor to promote the myosin II activity and cell traction force²⁸. (Supplementary Fig. 5A, 5B) After 24 h treatment, the magnitude of force could apparently attenuate senescence-associated biomarkers including p16^{INK4a}, p53, and p21^{WAF1/Cip1} (Fig. 3C and Supplementary Fig. 6B, 6D). The SA- β -gal staining coincided with the changes in these biomarkers, confirming the truth of enhancing mechanotransduction of aged cells might rejuvenate senescence to a certain extent (Fig. 3D).

One important hallmark of aging is replicative exhaustion of stem cell pools, thus the influence of mechanotransduction on cell proliferation was investigated via implementing ki67 staining and CCK8 assays. The results indicated that reducing cellular mechanotransduction of model cells could lower proliferative capacity and result in poor survival. Meanwhile, senescent cells had completely different performances, restoring cellular force with calyculin A promoted cell proliferation to great extent. (Fig. 3E, 3F). These data suggest that cellular mechanotransduction participates in the aging process, which not only influenced senescence-related biomarkers, but also affected the proliferative capacity of BMSCs.

To improve the reliability of this part, the experiment was also carried out with the bone marrow mesenchymal stromal cells from mice, and the data was consistent with the results in human stem cells. The decline in cellular force of young stem cells urged aging process, whereas upregulating the mechanotransduction of senescent cells resulted in partial alleviation of cellular senescence phenotypes. (Supplementary Fig. 7).

Above all, cellular mechanotransduction participates and performs as a regulator in aging process. The recovery of lost mechanotransduction could revive senescent cells, whereas the loss of it could cause the dysfunction of young cells.

Cellular mechanotransduction remodels chromatin accessibility.

The intracellular traction force and mechanotransduction have been reported to remodel the chromatin to regulate its accessibility and gene expression. This process is related to almost all the cell functions²⁹. The chromatin accessibility in young and senescent cells was thus systematically analyzed. Characterizing the chromatin state of cells by means of screening nucleus with confocal microscopy and calculating chromatin condensation parameters (CCP), we found that the decline in mechanical stimuli of young BMSCs showed overall more heterogeneous distributions of DAPI intensity, whereas elevating force of senescent cells altered chromatin remodeling and reduced the chromatin condensation in BMSCs (Fig. 4A, 4C).

The epigenetic regulator HDAC2 and HDAC3, which allow the histones to wrap the DNA and are regarded as useful negative markers of chromatin accessibility, were further investigated. The limited intracellular force triggered high expression of HDAC2 and HDAC3 in the senescent cells or the blebbistatin-treated young cells, while enhancing cellular force through calyculin A markedly decreased their expressions (Fig. 4B, 4D), supporting the conclusion that mechanical stimuli lead to a more open chromatin structure and higher levels of chromatin accessibility.

To further probe the chromatin accessible after the alteration of cellular force, genome-wide transposase-accessible chromatin sequencing (ATAC-seq) was employed in the study³⁰. Since chromatin landscape on gene promoters is associated with gene expression, firstly we analyzed differences in the chromatin accessibility over the transcription start site (TSS) and gene body (TES) as shown in Fig. 5A and 5B. We observed that all ATAC-seq samples were enriched for reads at transcription start sites (TSSs), however, gene promoters of senescent cells exhibited a strong decrease in chromatin accessibility, compared with the BMSCs from young donors. The young cells treated with blebbistatin had the analogous chromatin landscape like senescent cells. It uncovers that the decline in mechanotransduction represses the chromatin accessibility and induces the transcriptional disorders to trigger cellular senescence, which was in line with the CCP and HDAC analysis. Surprisingly, the senescent cells who underwent calyculin A treatment for 72 h had the smallest chromatin accessibility, which was ostensibly contradictory to all of the results with 24 h calyculin A treatment as shown above. The differentially accessible ATAC-seq peaks, as well as their enrichment, were also investigated. Differential analysis of ATAC-seq peaks revealed 36749 less accessible peaks of blebbistatin treatment for young cells, and simultaneously senescent cells treated with calyculin A also had 10338 downregulated peaks compared with the non-treated senescent cells, which were identical to the TSS results (Fig. 5C-E). The motif enrichment and KEGG enrichment analysis of differentially accessible ATAC-seq peaks showed that the blebbistatin treated young cells, the senescent cells, and the calyculin A treated senescent cells exhibited similar cell functions according to the analysis of the accessible chromatin regions (Fig. 5F, Supplementary Fig. 10A). In addition, based on the results of IGV Browser screenshot, the enrichment of ATAC-seq signals at the genes of LMNA (mechanotransduction factor) and MKI67 (proliferation marker) diminished visibly in senescent cells and blebbistatin-treated young cells, in contrast to the untreated cells from young donors, whereas exaltation of mechanotransduction with calyculin A had a minor impact on senescent cells among the signal enrichment of these genes (Fig. 5G, supplementary Fig. 10B). Therefore, the decline in cellular mechanotransduction repressed chromatin accessibility. The continuous treatment of senescent cells with calyculin A for 72 h closed chromatin, demonstrating the complex role of mechanical stimuli in the cell aging process. It seems mechanical stimuli may have negative effects on open chromatin landscape when it is beyond the endurance of senescent cells.

Mechanical overstimulation mitigates cellular mechanotransduction and accelerates cell senescence.

Whether the over-exposed mechanical stimuli accelerate cellular senescence and downregulate cell functions is attractive to be explored. The senescent BMSCs treated with calyculin A for 72 h gave rise to serious cellular senescence, compared with the same batch of cells without calyculin A treatment, which

were assayed by p16^{INK4a} expression, SA- β -gal staining, and p21^{WAF1/Cip1} expression (Fig. 6A-C). To exclude the toxicity and other side effects of calyculin A treatment, the mechanical stretching with frequencies of 0.02 Hz and 0.1 Hz (in the range to promote cell mechanotransduction)³¹ was performed on the senescent BMSCs. The results indicated by p16 and p53 detection supported the calyculin A treatment, where cells underwent reversed senescence at 0.02 Hz but accelerated senescence at 0.1 Hz (Fig. 6E). These data suggested that cellular force acts as a double-edged sword, with both beneficial and detrimental effects on the aging process, depending on the duration and intensity of the mechanical stimuli. Once the dose of force is out of range where BMSCs could sustain, it could lead to irreversible changes in cellular senescence. Our data establish a complicated role for cellular mechanotransduction in modulating the phenotypes of stem cell senescence.

The cellular mechanics and mechanotransduction under long-term calyculin A treatment were also monitored. The measurement of nanoindentation showed that the cells dealt with calyculin A had an obvious increase in Young's modulus during the first 24 h but a rapid decrease afterwards (Fig. 6D). The cell mechanics mirrored cytoskeleton assembly and intracellular force. The mechanical stretching promoted the level of P-myosin IIa at 0.02 Hz, while limited P-myosin IIa levels at 0.1 Hz (Supplementary Fig. 5C). The reason for the decrease of mechanotransduction and the effects on cell functions under long-term and intense mechanical stimuli must be thus explored. However, it seems the decreased mechanotransduction and intracellular force cause chromatin close to limit cell activity for cell aging.

DNA damage crosstalk with cellular mechanotransduction.

To further explore why mechanotransduction is decreased in senescent BMSCs, we paid attention to DNA damage, which could cause genome-wide transcriptional changes and initiate irreversible senescence and play a critical role in regulating the process discussed above. To test our hypothesis, we induced two DNA damage models including ultraviolet irradiation³² for 15 min and D-galactose exposure³³ for 48 h, both of which could obviously activate γ H2AX foci in young BMSCs (Supplementary Fig. 8). It has been shown that phosphorylation of H2AX is a major response to DNA damage, which localizes to damaged DNA and recruits DNA repair effectors to these sites³⁴. The DNA damage induced by either ultraviolet irradiation or D-galactose regulated mechanotransduction activity, as determined by immunofluorescence assays and western-blot assay with myosin IIa, P-myosin IIa, and Lamin A/C (Fig. 7A, 7B).

As mentioned above, we have already found multiple lines of evidence correlating cellular mechanotransduction with DNA damage. We then wonder whether, mechanistically, cellular force could promote the accumulation of DNA damage. To change cellular mechanotransduction, BMSCs were exposed to blebbistatin or calyculin A. Interestingly, the cellular force also regulates DNA damage. The γ H2AX was significantly reduced in BMSCs that were deficient in mechanotransduction due to blebbistatin treatment, indicating that the impairment of cellular mechanotransduction curbed sustained γ H2AX foci formation. Concomitantly, γ H2AX foci formation raised significantly after exposure to calyculin A for 72 h (Fig. 7C, and Supplementary Fig. 9A). The senescent cells were also cultured on the soft hydrogels (1.5 kPa) to test the DNA damage accrual. Consistent with the results of cells dealt with

blebbistatin, γ H2AX foci formation is markedly eliminated by culturing on the soft hydrogels (Fig. 7E). The comet assay³⁵ was further performed to confirm the DNA damage level. The suppression of cellular force was accompanied by limited tail DNA percent and tail moment length in BMSCs, indicating less DNA damage. Whereas, consistent with the increased γ H2AX foci formation after exposure to calyculin A, tail DNA percent and tail moment length was remarkably enhanced with calyculin A treatment for 72 h in senescent cells (Fig. 7D and Supplementary Fig. 9B). It suggests that cellular mechanotransduction may be an effective candidate for inducing DNA lesions. The mechanical overstimulation leads to more DNA damage, which then negatively regulates cell mechanotransduction. The next question is the function of this crosstalk for cellular senescence.

Mechanotransduction downregulation prevents DNA damage.

The evidence above suggests that the intracellular force, could open chromatin and increase DNA damage in the senescent cells. The reasonable hypothesis is that the downregulated mechanotransduction may close chromatin to prevent the DNA from suffering from further damage. The senescent cells were firstly treated with blebbistatin for 24 h to increase the chromatin condensation level. The cells were then irradiated by ultraviolet for 5–30 min in the presence of blebbistatin followed by DNA damage analysis after 24 h culturing without blebbistatin. We observed a statistically decline in DNA damage following ultraviolet irradiation for different times in mechanotransduction-deficient BMSCs, by applying a comet assay. The compromised tail DNA percent and tail moment length upon blebbistatin treatment occurred in each ultraviolet irradiated group, compared with in the absence of blebbistatin treatment (Fig. 8A,8B).

The soft hydrogels were also utilized to limit cellular mechanotransduction and intracellular force. The BMSCs were cultured on the soft hydrogels for 24 h, and then underwent ultraviolet irradiation for 15 min. After cells were transferred to cell culture plates for regular growth for 24 h, the DNA damage marker γ H2AX, proliferation marker ki67, and the mechanotransduction marker P-myosin IIa were examined (Fig. 8D). For comparison, the cells were cultured on the rigid plate for the same time and suffered the same ultraviolet irradiation. The data (Fig. 8E) showed that the impairment of mechanotransduction by soft hydrogels for 24 h is sufficient to counteract the lesions induced by DNA damage, as measured by the diminished accumulation of nuclear γ H2AX foci, which coincided with the benefit of decreasing mechanical stimuli by means of blebbistatin. Simultaneously, these protected cells were accompanied with higher proliferative capacity as detected by Ki67. The softening also prevented the DNA damage-induced cell force decline as marked by P-myosin IIa. The mechanotransduction activity was recovered after transferring the cells to the rigid plates, indicating the healthy state of the cells.

To better strengthen our conclusion, calyculin A was used to perform the opposite experiments. The senescent BMSCs were treated with calyculin A for 24 h and then stimulated by ultraviolet for 15 min in the presence of calyculin A. The nuclear γ H2AX foci formation was markedly heightened with calyculin A treatment (Fig. 8C), suggesting that the force-induced chromatin open caused DNA damage.

Taken together, these results suggest that the cellular mechanotransduction responds to DNA damage to close chromatin, which in turn prevents cells from suffering further lesions, creating protective feedback for cells. However, the closed chromatin leads to the decrease of the transcriptional activity of the force-downstream genes including growth, proliferation, and osteogenic differentiation^{36,37}, resulting in cell senescence.

Bone marrow tissue shows decreased mechanotransduction activity in response to DNA damage.

To further study whether the phenomenon we observed in vitro also existed in vivo, the DNA damage model mice were developed through continuous injection of doxorubicin³⁸ or D-galactose³⁹. These drugs could induce reactive oxygen species (ROS) accumulation and then trigger DNA damage in mice, and the efficiency was verified via detecting the γ H2AX (Fig. 9D). The DNA damage obviously diminished the level of mechanotransduction factors P-FAK and YAP, as compared to the untreated mice (Fig. 9A, 9B), which further induced aging as detected by P16 (Fig. 9C).

Discussion

In the present study, mechanotransduction has been proven to play an essential role during BMSC aging. Very recently, Piccolo group recognized YAP/TAZ as the key factors in the cell senescence⁴⁰. As YAP/TAZ are the direct sensors and regulators in mechanotransduction²⁶, their and our studies can confirm each other. We have further unraveled the causative event and the mechanism via which mechanotransduction takes part in aging process and verified the complexity and systematicity of the crosstalk between mechanotransduction and aging process. The data presented here show that although the decline in cellular mechanotransduction contributes to the impaired proliferation capacity in aged cells by acting as a chromatin accessibility regulator, it also provides self-protection to prevent further DNA damage, highlighting its importance in the regulation of DNA damage-chromatin remodeling-cellular senescence axis (Fig. 10).

We verified that, upon aging, there is an obvious downregulation of cellular mechanotransduction in senescent BMSCs, and strikingly, restoring the mechanotransduction temporarily decreases senescence-related biomarkers. Particularly, when mechanical stimuli are accumulated, it could induce cellular senescence. The reason is that the over-opened chromatin triggers intensive DNA lesions, which in turn reduces cellular mechanotransduction pathways.

Numerous studies have proved that force could induce nucleus deformation^{29,41} and modulate chromatin landscape, thereby influencing epigenetic modifications and gene expression^{42,43}. Therefore, investigating the crosstalk between cellular mechanotransduction and DNA damage is of great importance, particularly in the context of aging, in which cellular chromatin accessibility undergoes profound alterations and gene expression profiles are dynamic⁴⁴. Our data clearly indicate that DNA damage could lower cellular mechanotransduction to a great extent, which could explain the phenomenon that why low-level mechanotransduction occurs upon cellular senescence. It will be

interesting to further assess whether the decreased force in senescent cells is a universal mechanism across cell types, identifying its utility as markers and potential therapeutic targets. This discovery might be helpful for compensating the deficiency in senescence targets in the field of aging research.

In recent years, some studies use some kinds of methods to treat age-associated diseases, of which defining senescent cells and then getting rid of them is a popular therapeutic strategy^{7,45}, however, it is challenging to rescue the function of the senescent cells. We have attempted to rejuvenate them through the re-establishment of the mechanical stimuli system. The low levels of the mechanical stimuli performed on the aged BMSCs resulted in decreased senescence-related biomarkers and temporarily restored cell proliferation capacity due to enhanced chromatin accessibility and gene transcription. It might be considered in antiaging treatment to improve the therapeutic outcomes of age-related bone loss.

The appropriate force is critical for maintaining fundamental cellular biological function and downregulation of mechanotransduction drives cell aging by controlling chromatin landscape. Meanwhile, the high levels of mechanical stimuli accelerate DNA lesions and cell aging. Since the levels of the individual cellular senescence and their tolerance are quite diverse, it is difficult to normalize the mechanical stimuli's standards and the precise details should be the subject of future studies.

Above all, an important contribution of decreased cellular mechanotransduction in aged cells is starting to emerge with a series of our results, demonstrating that this behavior acts as a good self-protection mechanism via which senescent cells avoid further DNA damage, so it is the art of senescent cell survival.

Our findings provide insights into how mechanotransduction affects aging-associated processes including DNA damage and cellular senescence, thereby uncovering the causes, the rationality, and the significance of age-related alterations of mechanotransduction in senescent cells.

Methods

Mice. Male C57BL/6 mice aged 6 weeks were utilized as the young group and their counterparts of 20 months were accepted as the naturally aged group.

As for the induced DNA damage mouse model, both doxorubicin and D-Galactose were used respectively in our study. Doxorubicin (Sigma, USA) or D-Galactose (Solarbio, China) was dissolved in saline at the concentration of 100mg/ml and then sterilized using a 0.22 μ m filter. The mice (C57bl/6, male) aged 6 weeks were administered with Dox at 5 mg/kg via intraperitoneal injection once a week for 4 weeks. Simultaneously, D-gal was injected subcutaneously daily at a dose of 500 mg/kg body weight for 3 months and the control group was injected with saline at an equivalent dose. All animal experiments were performed approved by the Ethics Committee at West China Hospital of Stomatology, Sichuan University.

Micro CT tomography evaluation. The femurs from aged and young mice were measured using micro-CT. SkyScan 1176 desktop X-ray Micro-CT system (Skyscan, Bruker) (0.5 mm Al filter, image pixel size: 17.75

µm, voltage: 60 kV, electrical current:400 µA) was used to scan the target regions. The exposure time was 1080 ms.

Histological analyses. Histological analyses were used to detect the differences between the tissue from aged and young mice via immunohistochemistry and Masson staining according to the protocol. The dissected femurs were fixed in 4% paraformaldehyde for 2 days and then decalcified in 12% EDTA for 1 week. Slides were subjected to sodium citrate buffer at 99°C for 20min for antigen retrieval and then incubated with rabbit polyclonal anti-collagen I (1:800, Servicebio, Cat No: GB11022-3), rabbit anti-phospho-FAK (1:50, Thermo Fisher Scientific, Cat No:700255), rabbit polyclonal anti-YAP (1:100, Genxspan, Cat No: GXP539020), rabbit polyclonal anti-P16 (1:100, Invitrogen, Cat No: PA1-30670) and rabbit polyclonal anti-phospho-Histone H2A.X (ser139) (1:100, Cell Signaling Technology, Cat No: 9718). Then anti-rabbit IgG antibody was used as secondary antibodies (1:200). For Masson staining, the tissue was stained by Masson (Solarbio, China) staining solution according to the instruction. Images were captured using a microscope (Olympus, Japan).

Cell culture. Bone marrow aspirates from old (60 ~ 80 years old) and young (18 ~ 30 years old) were obtained from healthy patients who were firstly suspected of having hematological diseases at West China Hospital of Sichuan University. After that, per milliliter of bone marrow was plated on T-75 flasks using a medium supplemented with 10% fetal bovine serum (Gibco) and 0.01% penicillin/streptomycin. Medium renewal was implemented every 3 days. We performed cell sorting using flow cytometry at day 12 and passages between 3 to 5 were accepted for subsequent experiments. BMSCs from three independent donors among each age group (aged vs. young) were mixed and utilized together in the study. The experiment was approved by the Ethics Committee of West China Hospital of Stomatology, Sichuan University.

For BMSCs derived from mice, 20-month mice and their counterpart aged 6-week-old were used in our experiments and we finished this part according to our previous protocol⁴⁶. Firstly, we dislocated the femur and cut off both ends under aseptic conditions. Then intact bone marrow was isolated, blown into pieces, and seeded in 100 mm diameter Petri dishes. The cells were cultured in the same condition as BMSCs derived from humans. Cells at the passage between 2 to 4 were adopted for subsequent experiments.

Clonal expansion. The colony formation assay was employed to assess self-renewal ability of BMSCs from different ages. Senescent and young cells at the density of 1×10^3 cells/well were inoculated in 6-well plates for 12 days. The colony formation was detected by crystal violet (Solarbio, China) staining according to the manufacturer's instructions.

Alizarin red staining and Oil Red O staining. For osteogenic differentiation, BMSC were cultured on 24-well plates and underwent osteogenic induction for 14 days, after that, alizarin red staining was performed with Alizarin red solution (Sigma). For evaluating the lipid droplet formation, Oil Red O staining was performed with a kit from Diagnostic Biosystems (Cat No: KT025) after 14 days of adipogenic induction.

Nanoindentation. Nano-indentation was used to measure young's modulus of young and senescent BMSCs, which was determined by fitting force-indentation curves to known models according to the manufacturer's instructions. The diameter of the nano-indentation indenter is 10.5 μm , the stiffness of the indenter is 0.05 N/m, and the indentation depth is 3 μm in our research.

Traction force microscopy (TFM). Traction force microscopy was used to detect cellular mechanotransduction according to our previous protocol⁴⁷. Firstly, PEG hydrogels containing 0.5 μm fluorescent carboxylated polystyrene beads (Sigma) were fabricated and the micro-beads existed at the surface of the hydrogels. After hydrogels were soaked for 48 h, seeding young and senescent MSCs on the PEG hydrogels. A confocal microscope was exploited to take images of beads and the spreading area of cells, regarding as the shifted position of beads induced by cell migration. Finally, both young and senescent cells were cleared up by dealing with 1% SDS and taken photos afterwards.

Quantification of fiber's anisotropy. FibrilTool, a plugin of ImageJ, was introduced to quantify the orientation of fibrillar structures in the studies according to the protocol. After capturing the pictures of β -actin, we calculated the anisotropy of young and senescent cells respectively, in order to compare the differences in cellular mechanical characteristics. Regarding the anisotropy score, the following convention: 0 for no order (purely isotropic arrays) and 1 for perfectly ordered (purely anisotropic arrays) were used. Another plugin of ImageJ named Orientation J was also used to measure the orientation of the fiber where the color representation reflects the different orientations.

Immunofluorescence and confocal microscopy. Cells were fixed for 15 min at 37°C with 4% paraformaldehyde, permeabilized with 1% Triton-X100 (Sigma) for 15 min and blocked with 5% BSA diluted in PBS for 15 min at RT. BMSCs were then incubated, overnight at 4°C with the indicated primary antibodies in 1% BSA. The following antibodies were used: Myosin IIa (1:100, Cell Signaling Technology, Cat No:3403), phospho-Myosin IIa (1:200, Cell Signaling Technology, Cat No:14611), Lamin A/C (1:200, Cell Signaling Technology, Cat No:4777), YAP (1:100, Cell Signaling Technology, Cat No:14074), phospho-Histone H2A.X (ser139) (1:200, Cell Signaling Technology, Cat No: 9718), P16 (1:200, Invitrogen, Cat No: PA1-30670), p21(1:200, Cell Signaling Technology, Cat No:2947), P53 (1:100, Cell Signaling Technology, Cat No:2524), HDAC2 (1:200, Santa Cruz Biotechnology, Cat SC-9959), HDAC3(1:200, Cell Signaling Technology, Cat No:3949) and ki67(1:200, Abcam, ab15580). Following this, cells were incubated for 2h at 4°C with the appropriate secondary fluorescent antibodies diluted in 1% BSA, protected from light. At last, nuclei were stained with DAPI (1:1000, Solarbio, China). Images were collected under a confocal laser scanning microscope (CLSM, Olympus, Japan).

Western blot experiments. BMSCs were seeded in six-well plates and treated with different conditions for different time. Then the experiment was finished according to our reported protocol⁴⁸. Protein concentration was determined using the BCA Protein Assay Kit (Bio-Rad, U.S.), and then 30 μg of total protein was run on 8%-12% SDS-PAGE gel (Beyotime, Shanghai, China), and electro-transferred to polyvinylidene difluoride (PVDF) membranes (Millipore) for 2h-3h at 120 mA in transfer buffer. The following antibodies were used: Myosin II a, phospho-Myosin IIa, Lamin A/C, p21, and β -actin. The

concentration of these antibodies in this experiment was 1:1000. After three 10-min washes with TBST, membranes were incubated with the appropriate secondary antibody (1:5000) for 1 h at room temperature. Immunoreactive bands were visualized by a western lightning chemiluminescence detection kit (Zen Bioscience, China).

Senescence-Associated β -Galactosidase (SA- β -Gal) Staining. Senescent cells were measured by use of the SA- β -gal staining kit (Solarbio, China) according to previous reported⁴⁶. After incubated with the reagent about 8 h-12 h, senescent cells would be stained with aquamarine blue, whereas young cells were not able to be colored.

Cell proliferation assay. To investigate the effect of cellular mechanotransduction on BMSC proliferation, CCK-8 (Solarbio, China) was implemented in the study. Briefly, BMSCs were seeded into 96-well plates and cultured overnight. After that, young and senescent cells were treated with blebbistatin and calyculin A for 24 h respectively, and then incubated with CCK-8 reagent for analysis as previous reported⁴⁶.

ATAC-seq and analyses. ATAC-seq were prepared according to the protocol of Novogene (Beijing, China). The details were showed in the supplementary information.

Comet assay. Comet assay was performed by use of the Cell Biolabs kit (San Diego, USA, Cat No: STA-350). Briefly, cells were dealt with blebbistatin or calyculin A for 72 h and resuspended at a concentration of 1×10^5 cells/ml. Cell suspensions were mixed with low melting agarose, and then were transferred to the supplied glass slides at 4°C for 15 min. After that, cell lysis was carried out and electrophoresis was employed in a tank containing the alkaline running buffer at electric current of 300 mA for 30 min. The slides were stained with SYBR Gold Nucleic Acid Gel Stain (Invitrogen, Cat No: S11494) for 10 min. Images were acquired using a confocal laser scanning microscope. To compare DNA damage in different groups, tail moment length, and tail DNA percent were quantified using an open comet software plugin in FIJI.

Statistical analysis. All data were presented as mean \pm SD. Prism 8.0.1 (GraphPad Software) was used for the two-tailed Student's t-test. *, $P < 0.05$, **, $P < 0.01$, ***, $P < 0.001$ were considered statistically significant.

Declarations

Fundings:

This work is financially sponsored by financial support from the National Key Research and Development Program of China (2021YFA1100600) and the National Natural Science Foundation of China (Grant No. 32000951, 51973129, 82071092, U21A20369).

Authors' contributions:

Xiaojing Liu performed the experiments, analyzed the results, and wrote the manuscript. Li Liao initiated the project, co-supervised the project, analyzed the results, and revised the manuscript. Peng Wang assisted the detection of cellular mechanotransduction. Yuanxin Ye was responsible for human bone marrow collection. Xiangyu Dong assisted the cell mechanics measurement. Xiaotao Xing helped in vivo experiments. Zhonghan Li helped to design the experiments, discuss the results, and revised the manuscript. Qiang Wei conceived the idea, designed the research, analyzed the results, and wrote the manuscript. Weidong Tian supervised the project and provides financial support. All authors reviewed and approved the final manuscript.

Conflict of interest:

The authors declare no competing interests.

References

1. Marie, P. J. & Kassem, M. Extrinsic mechanisms involved in age-related defective bone formation. *J Clin Endocrinol Metab* **96**, 600–609, doi:10.1210/jc.2010-2113 (2011).
2. Kassem, M. & Marie, P. J. Senescence-associated intrinsic mechanisms of osteoblast dysfunctions. *Aging Cell* **10**, 191–197, doi:10.1111/j.1474-9726.2011.00669.x (2011).
3. Langdahl, B., Ferrari, S. & Dempster, D. W. Bone modeling and remodeling: potential as therapeutic targets for the treatment of osteoporosis. *Ther Adv Musculoskelet Dis* **8**, 225–235, doi:10.1177/1759720X16670154 (2016).
4. Saidak, Z. & Marie, P. J. Strontium signaling: molecular mechanisms and therapeutic implications in osteoporosis. *Pharmacol Ther* **136**, 216–226, doi:10.1016/j.pharmthera.2012.07.009 (2012).
5. Burr, D. B. & Gallant, M. A. Bone remodelling in osteoarthritis. *Nat Rev Rheumatol* **8**, 665–673, doi:10.1038/nrrheum.2012.130 (2012).
6. Calcinotto, A. *et al.* Cellular Senescence: Aging, Cancer, and Injury. *Physiol. Rev.* **99**, 1047–1078, doi:10.1152/physrev.00020.2018 (2019).
7. Di Micco, R., Krizhanovsky, V., Baker, D. & d'Adda di Fagagna, F. Cellular senescence in ageing: from mechanisms to therapeutic opportunities. *Nat. Rev. Mol. Cell Biol.* **22**, 75–95, doi:10.1038/s41580-020-00314-w (2021).
8. van Deursen, J. M. The role of senescent cells in ageing. *Nature* **509**, 439–446, doi:10.1038/nature13193 (2014).
9. Schumacher, B., Pothof, J., Vijg, J. & Hoeijmakers, J. H. J. The central role of DNA damage in the ageing process. *Nature* **592**, 695–703, doi:10.1038/s41586-021-03307-7 (2021).
10. Kang, C. *et al.* The DNA damage response induces inflammation and senescence by inhibiting autophagy of GATA4. *Science* **349**, aaa5612, doi:10.1126/science.aaa5612 (2015).
11. Lopez-Otin, C., Blasco, M. A., Partridge, L., Serrano, M. & Kroemer, G. The hallmarks of aging. *Cell* **153**, 1194–1217, doi:10.1016/j.cell.2013.05.039 (2013).

12. Iskratsch, T., Wolfenson, H. & Sheetz, M. P. Appreciating force and shape—the rise of mechanotransduction in cell biology. *Nat. Rev. Mol. Cell Biol.* **15**, 825–833, doi:10.1038/nrm3903 (2014).
13. Koester, J. *et al.* Niche stiffening compromises hair follicle stem cell potential during ageing by reducing bivalent promoter accessibility. *Nat. Cell Biol.* **23**, 771–781, doi:10.1038/s41556-021-00705-x (2021).
14. Martyniak, K. *et al.* Do polyunsaturated fatty acids protect against bone loss in our aging and osteoporotic population? *Bone* **143**, 115736, doi:10.1016/j.bone.2020.115736 (2021).
15. Heisenberg, C. P. & Bellaïche, Y. Forces in tissue morphogenesis and patterning. *Cell* **153**, 948–962, doi:10.1016/j.cell.2013.05.008 (2013).
16. Vining, K. H. & Mooney, D. J. Mechanical forces direct stem cell behaviour in development and regeneration. *Nat Rev Mol Cell Biol* **18**, 728–742, doi:10.1038/nrm.2017.108 (2017).
17. Halder, G., Dupont, S. & Piccolo, S. Transduction of mechanical and cytoskeletal cues by YAP and TAZ. *Nat Rev Mol Cell Biol* **13**, 591–600, doi:10.1038/nrm3416 (2012).
18. Wen, J. H. *et al.* Interplay of matrix stiffness and protein tethering in stem cell differentiation. *Nat. Mater.* **13**, 979–987, doi:10.1038/nmat4051 (2014).
19. Wolf, K. *et al.* Physical limits of cell migration: control by ECM space and nuclear deformation and tuning by proteolysis and traction force. *J Cell Biol* **201**, 1069–1084, doi:10.1083/jcb.201210152 (2013).
20. Pegoraro, G. *et al.* Ageing-related chromatin defects through loss of the NURD complex. *Nat Cell Biol* **11**, 1261–1267, doi:10.1038/ncb1971 (2009).
21. Parry, A. J. *et al.* NOTCH-mediated non-cell autonomous regulation of chromatin structure during senescence. *Nat Commun* **9**, 1840, doi:10.1038/s41467-018-04283-9 (2018).
22. Niedernhofer, L. J. *et al.* Nuclear Genomic Instability and Aging. *Annu Rev Biochem* **87**, 295–322, doi:10.1146/annurev-biochem-062917-012239 (2018).
23. González, S. *et al.* Mechanotransduction and epigenetic control in autoimmune diseases. *Autoimmunity Reviews* **10**, 175–179, doi:10.1016/j.autrev.2010.09.022 (2011).
24. Dupont, S. & Wickstrom, S. A. Mechanical regulation of chromatin and transcription. *Nat. Rev. Genet.*, doi:10.1038/s41576-022-00493-6 (2022).
25. Hamadi, A. *et al.* Regulation of focal adhesion dynamics and disassembly by phosphorylation of FAK at tyrosine 397. *J Cell Sci* **118**, 4415–4425, doi:10.1242/jcs.02565 (2005).
26. Dupont, S. *et al.* Role of YAP/TAZ in mechanotransduction. *Nature* **474**, 179–183, doi:10.1038/nature10137 (2011).
27. Boudaoud, A. *et al.* FibrilTool, an ImageJ plug-in to quantify fibrillar structures in raw microscopy images. *Nat Protoc* **9**, 457–463, doi:10.1038/nprot.2014.024 (2014).
28. Hou, Y. *et al.* Surface Roughness and Substrate Stiffness Synergize To Drive Cellular Mechanoresponse. *Nano Lett.* **20**, 748–757, doi:10.1021/acs.nanolett.9b04761 (2020).

29. Tajik, A. *et al.* Transcription upregulation via force-induced direct stretching of chromatin. *Nat Mater* **15**, 1287–1296, doi:10.1038/nmat4729 (2016).
30. Buenrostro, J. D., Giresi, P. G., Zaba, L. C., Chang, H. Y. & Greenleaf, W. J. Transposition of native chromatin for fast and sensitive epigenomic profiling of open chromatin, DNA-binding proteins and nucleosome position. *Nat Methods* **10**, 1213–1218, doi:10.1038/nmeth.2688 (2013).
31. Andreu, I. *et al.* The force loading rate drives cell mechanosensing through both reinforcement and cytoskeletal softening. *Nat Commun* **12**, 4229, doi:10.1038/s41467-021-24383-3 (2021).
32. Xiang, Y. *et al.* RNA m(6)A methylation regulates the ultraviolet-induced DNA damage response. *Nature* **543**, 573–576, doi:10.1038/nature21671 (2017).
33. He, Z. H. *et al.* The nuclear transcription factor FoxG1 affects the sensitivity of mimetic aging hair cells to inflammation by regulating autophagy pathways. *Redox. Biol.* **28**, 101364, doi:10.1016/j.redox.2019.101364 (2020).
34. Ivashkevich, A., Redon, C. E., Nakamura, A. J., Martin, R. F. & Martin, O. A. Use of the gamma-H2AX assay to monitor DNA damage and repair in translational cancer research. *Cancer Lett* **327**, 123–133, doi:10.1016/j.canlet.2011.12.025 (2012).
35. Gyori, B. M., Venkatachalam, G., Thiagarajan, P. S., Hsu, D. & Clement, M. V. OpenComet: an automated tool for comet assay image analysis. *Redox. Biol.* **2**, 457–465, doi:10.1016/j.redox.2013.12.020 (2014).
36. Hu, Y., Kireev, I., Plutz, M., Ashourian, N. & Belmont, A. S. Large-scale chromatin structure of inducible genes: transcription on a condensed, linear template. *J Cell Biol* **185**, 87–100, doi:10.1083/jcb.200809196 (2009).
37. Carpenter, A. E., Memedula, S., Plutz, M. J. & Belmont, A. S. Common effects of acidic activators on large-scale chromatin structure and transcription. *Mol Cell Biol* **25**, 958–968, doi:10.1128/MCB.25.3.958-968.2005 (2005).
38. Sun, T. *et al.* Characterization of cellular senescence in doxorubicin-induced aging mice. *Exp Gerontol* **163**, 111800, doi:10.1016/j.exger.2022.111800 (2022).
39. Sun, S. W. *et al.* Quercetin attenuates spontaneous behavior and spatial memory impairment in d-galactose-treated mice by increasing brain antioxidant capacity. *Nutrition Research* **27**, 169–175, doi:10.1016/j.nutres.2007.01.010 (2007).
40. Sladitschek-Martens, H. L. *et al.* YAP/TAZ activity in stromal cells prevents ageing by controlling cGAS-STING. *Nature* **607**, 790–798, doi:10.1038/s41586-022-04924-6 (2022).
41. Kim, D. H. & Wirtz, D. Cytoskeletal tension induces the polarized architecture of the nucleus. *Biomaterials* **48**, 161–172, doi:10.1016/j.biomaterials.2015.01.023 (2015).
42. Talwar, S., Jain, N. & Shivashankar, G. V. The regulation of gene expression during onset of differentiation by nuclear mechanical heterogeneity. *Biomaterials* **35**, 2411–2419, doi:10.1016/j.biomaterials.2013.12.010 (2014).
43. Ramdas, N. M. & Shivashankar, G. V. Cytoskeletal control of nuclear morphology and chromatin organization. *J Mol Biol* **427**, 695–706, doi:10.1016/j.jmb.2014.09.008 (2015).

44. Hernandez-Segura, A. *et al.* Unmasking Transcriptional Heterogeneity in Senescent Cells. *Curr Biol* **27**, 2652–2660 e2654, doi:10.1016/j.cub.2017.07.033 (2017).
45. He, S. & Sharpless, N. E. Senescence in Health and Disease. *Cell* **169**, 1000–1011, doi:10.1016/j.cell.2017.05.015 (2017).
46. Xing, X. *et al.* Local Elimination of Senescent Cells Promotes Bone Defect Repair during Aging. *ACS Appl. Mater. Interfaces* **14**, 3885–3899, doi:10.1021/acsami.1c22138 (2022).
47. Zhang, M. *et al.* Controllable ligand spacing stimulates cellular mechanotransduction and promotes stem cell osteogenic differentiation on soft hydrogels. *Biomaterials* **268**, 120543, doi:10.1016/j.biomaterials.2020.120543 (2021).
48. Liu, X. *et al.* EGFR-mediated signaling pathway influences the sensitivity of oral squamous cell carcinoma to JQ1. *J. Cell. Biochem.* **119**, 8368–8377, doi:10.1002/jcb.26920 (2018).

Figures

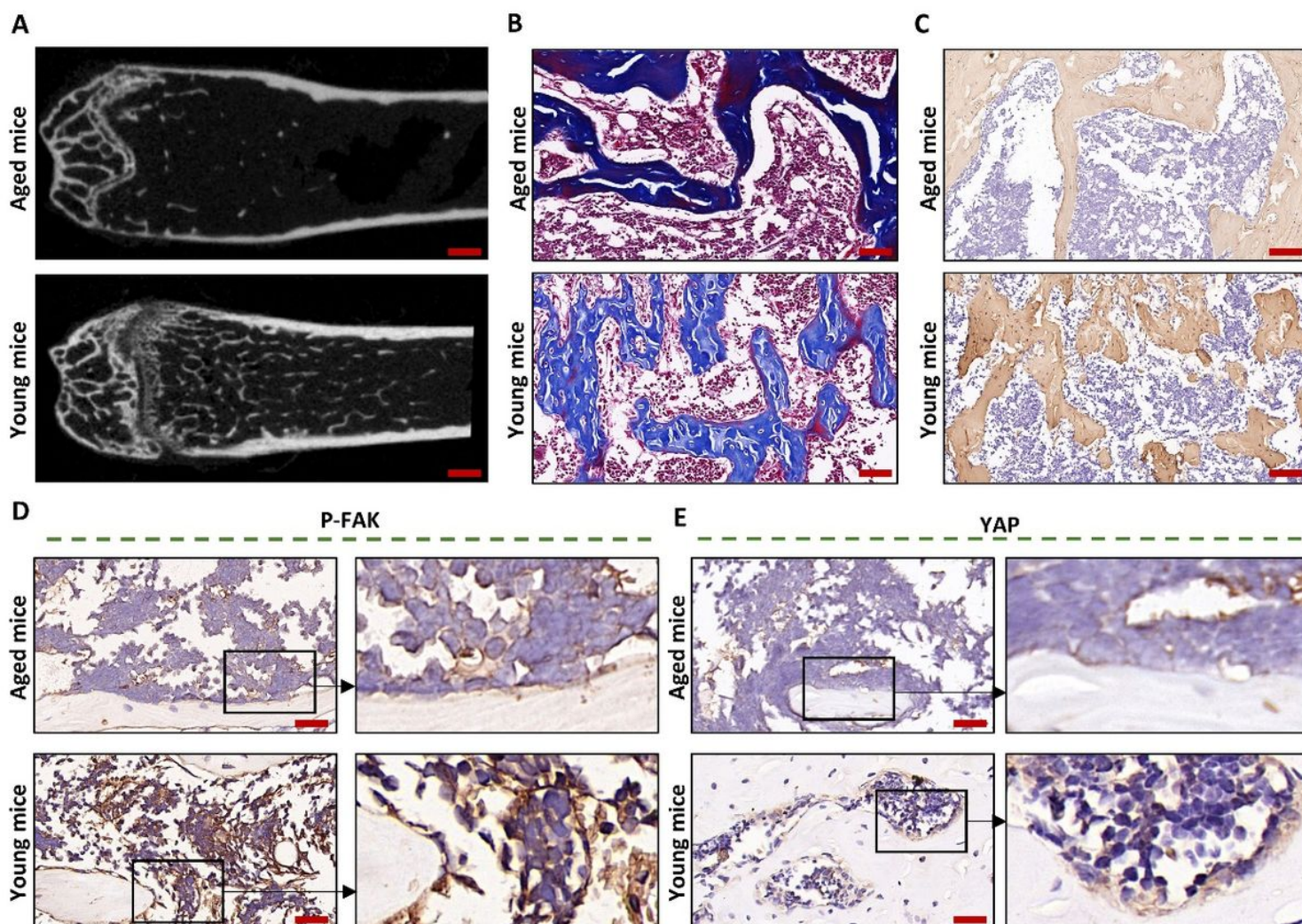


Figure 1

Bone marrow tissue of aged mice had variation in microarchitecture and mechanotransduction activity.

(A) Micro-CT showed that the 20-month mice had less trabecular numbers and greater trabecular spacing than 6-week mice. (Scale bar, 50 μ m) (B) Representative Masson staining of femurs from aged mice and young mice respectively. (C) Immunostaining showed downregulation of collagen I in aged mice than in young mice. (D) Immunostaining showed that p-FAK and (E) YAP was absent in old mice aged 20-month compared to in young mice aged 6-week. Right panel represents the magnified area of the red frame in the left panel (B-E, Scale bar, 100 μ m. n = 5)

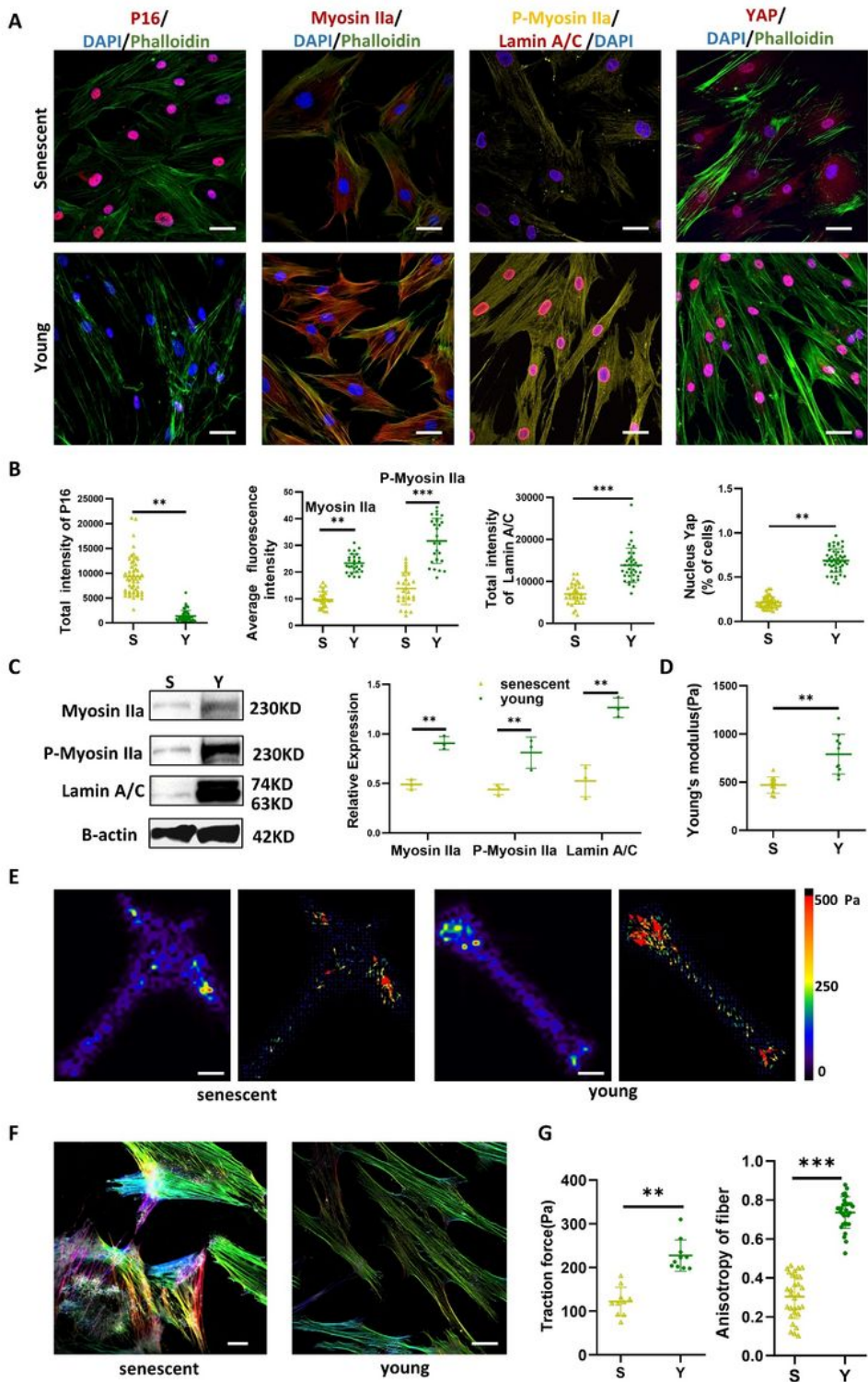


Figure 2

Cellular mechanotransduction decreases in senescent stem cells.

(A) Representative immunofluorescence staining and the (B) related quantification of the aging marker p16^{INK4a} and the mechanotransduction markers Myosin IIa, P-myosin IIa, Lamin A/C, and YAP nucleus localization. (C) Western blot analysis of mechanotransduction markers. (D) Nanoindentation results of

senescent and young BMSCs. (E) Representative figure of traction force microscopy measurement. (F) The anisotropy of actin stress fibers and the color representation reflect the different orientations. (G) The analysis of Fig E and Fig F. (Scale bar, 50 μm)

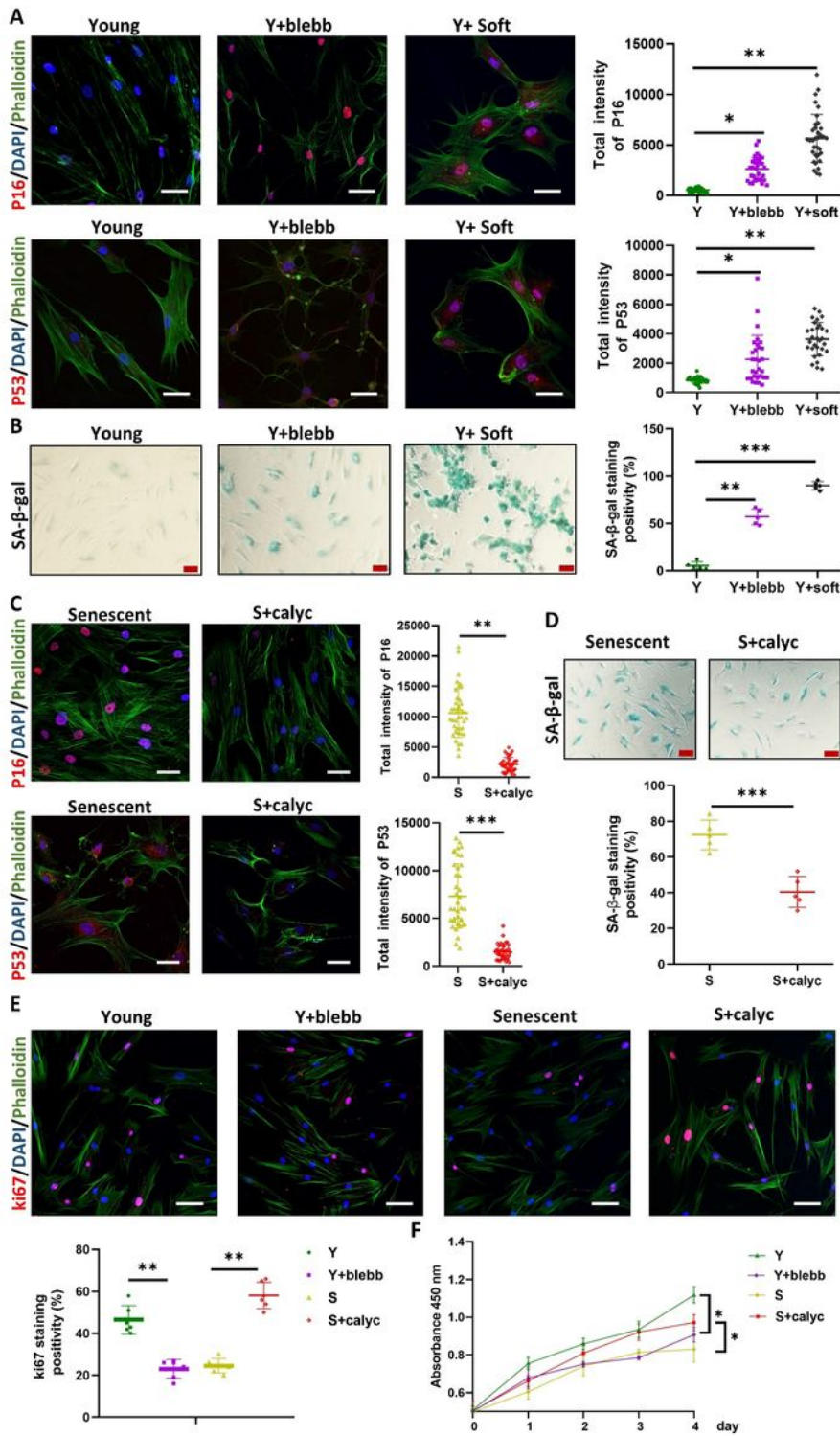


Figure 3

Cellular mechanotransduction regulates cell senescence and cell proliferation.

(A) Immunofluorescence analysis of p16 and p53 as well as (B) SA- β -gal staining after decreasing intracellular force of young BMSCs via blebbistatin or soft hydrogels for 24 h. (C) Immunofluorescence analysis of p16 and p53 as well as (D) SA- β -gal staining after increasing intracellular force of senescent BMSCs by calyculin A for 24 h. (E) Immunofluorescence staining of ki67 after young and senescent BMSCs treated with blebbistatin or calyculin A for 24 h respectively. (F) CCK-8 assays after cells were induced by different drugs. (Scale bar, 50 μ m)

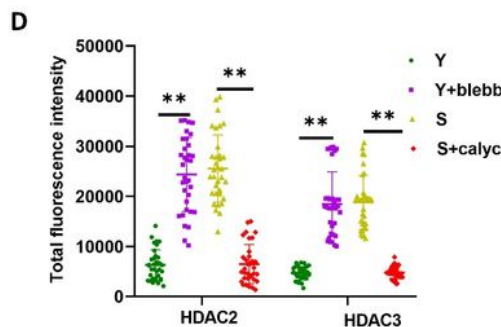
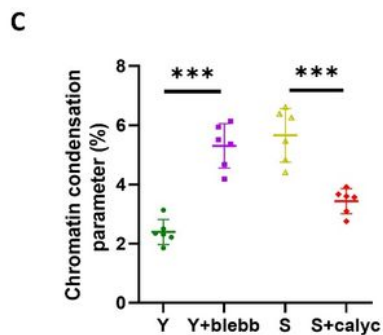
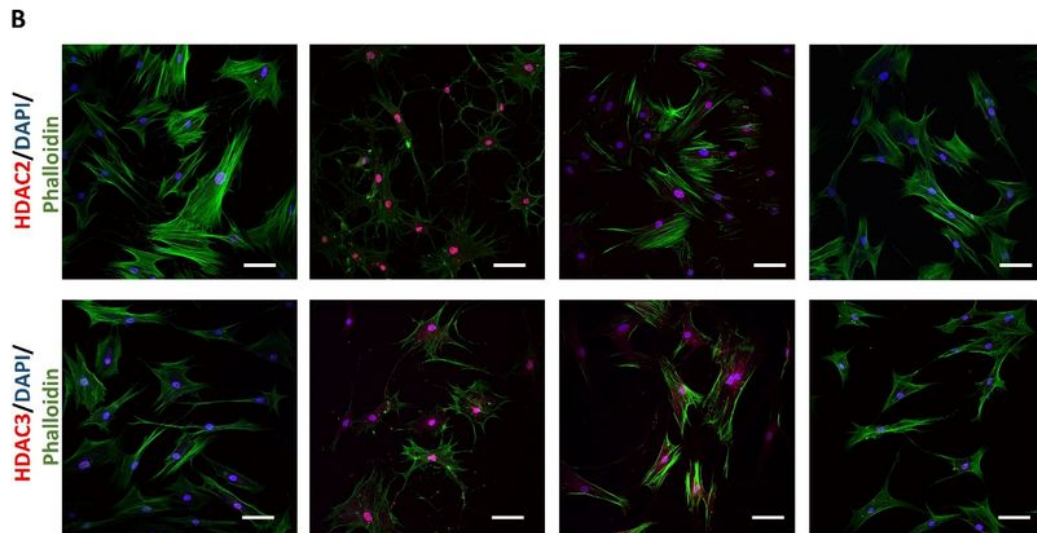
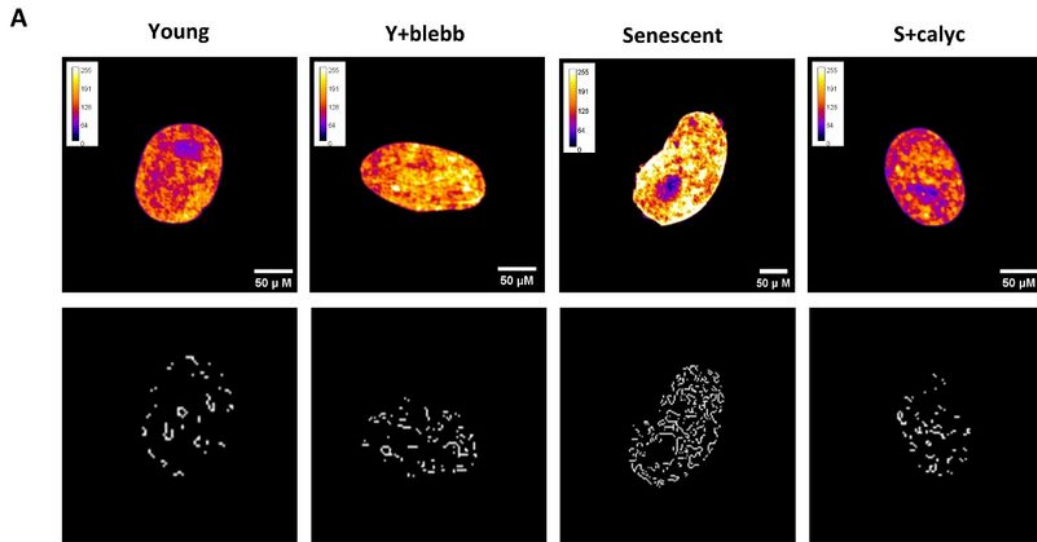


Figure 4

Cellular mechanotransduction remodels chromatin accessibility.

(A) Representative heatmaps of the DAPI fluorescence images and the chromatin condensation parameter (CCP) maps estimated by corresponding edge detection method for the cells treated with different drugs. (B) Immunofluorescence staining of HDAC2 and HDAC3 after young and senescent BMSCs were treated with blebbistatin or calyculin A, respectively. (C) Quantification of the average chromatin condensation parameters of the related cells. (D) Quantification of the immunofluorescence results of HDAC2 and HDAC3 from the related images. (Scale bar, 50 μm)

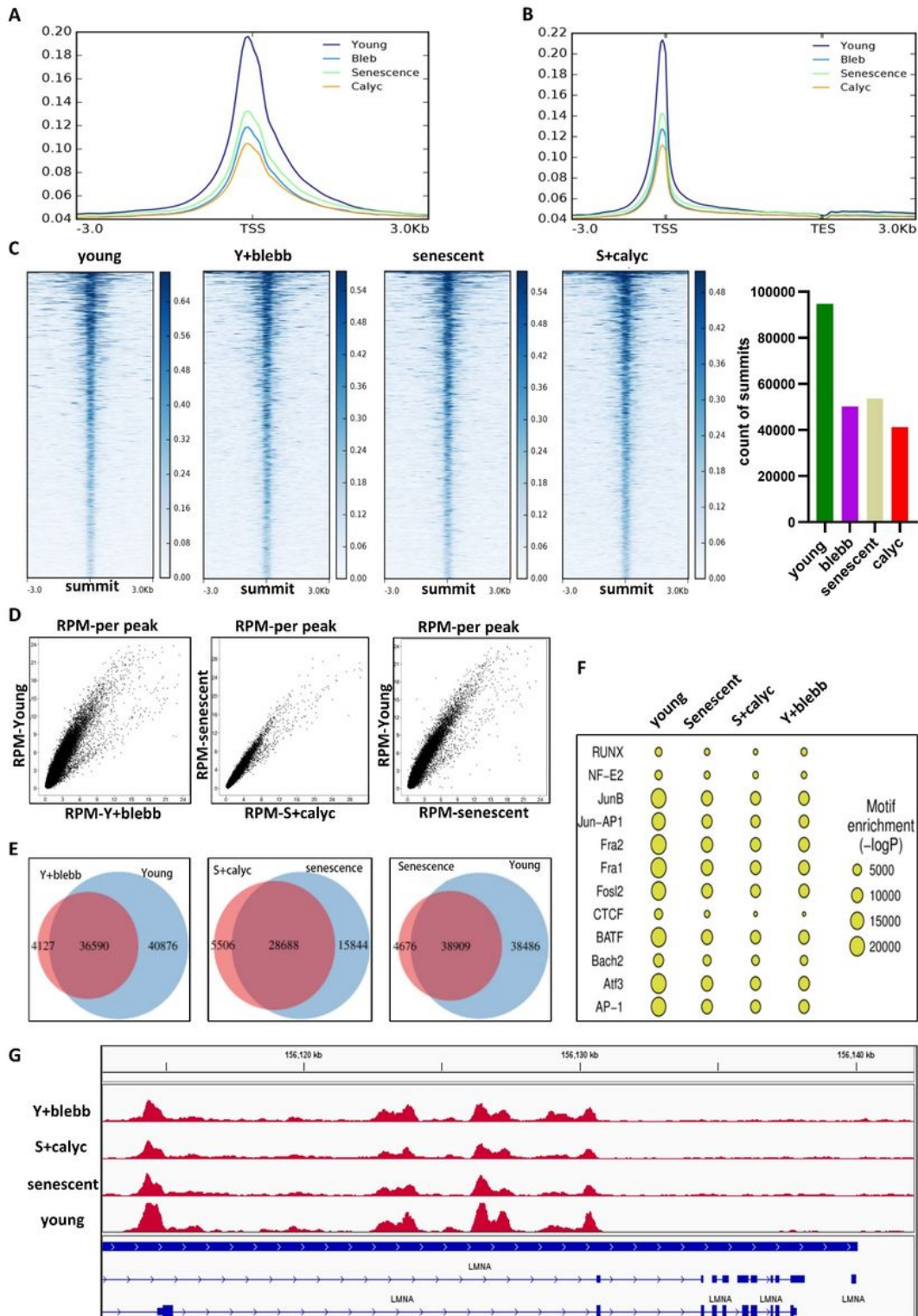


Figure 5

ATAC-seq results after altering cellular mechanotransduction by blebbistatin or calyculin A. (A) Metaplot of ATAC-seq reads over the TSS (transcription start Sites) and (B) TES (gene body). (C) Heat map of differentially accessible ATAC-seq peaks. Note the widespread reduction in chromatin accessibility in senescent cells, blebbistatin treated young cells, and calyculin A treated senescent BMSCs. (D) The enrichment of differentially accessible ATAC-seq peaks. (E) Differential ATAC-seq peaks among different

groups. (F) Motif enrichment of ATAC-seq peaks in each of the groups. (G) IGV browser views showing LMNA read density in young, senescent, blebbistatin treated young cells, and calyculin A treated senescent BMSCs.

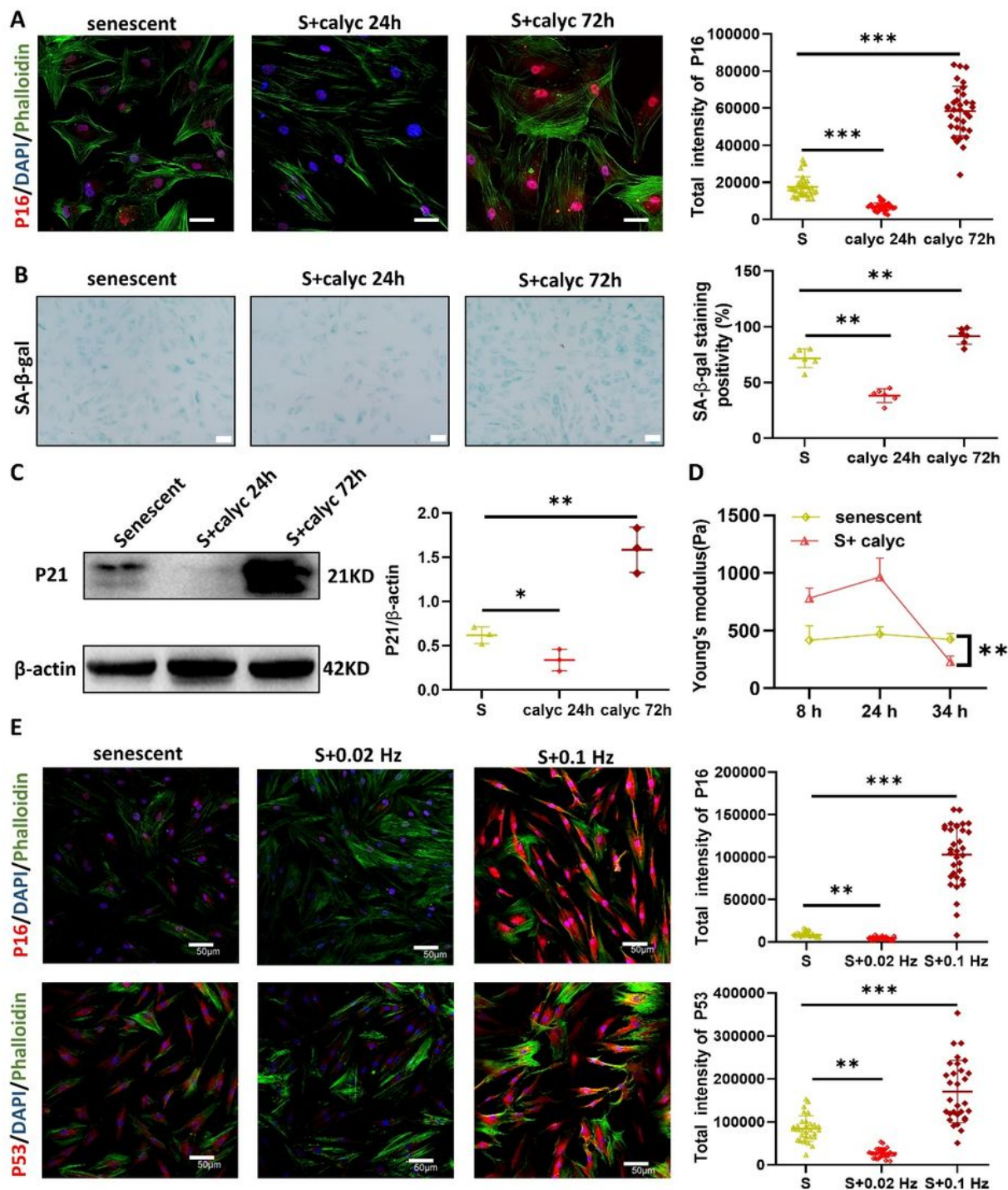


Figure 6

Mechanical overstimulation mitigates cellular mechanotransduction and accelerates cell senescence.

(A) Immunofluorescence staining of p16^{INK4a} after senescent BMSCs were treated by calyculin A for 24 h or 72 h. (B) SA- β -gal staining after calyculin A treatment for 24 h or 72 h. (C). Western blot analysis of P21 after calyculin A treatment for 24 h or 72 h. (D) The measurement of nanoindentation when cells were dealt with calyculin A for different times. (E) The expression of P16 and P53 after cells were treated with mechanical stretching at different frequencies. (Scale bar, 50 μ m)

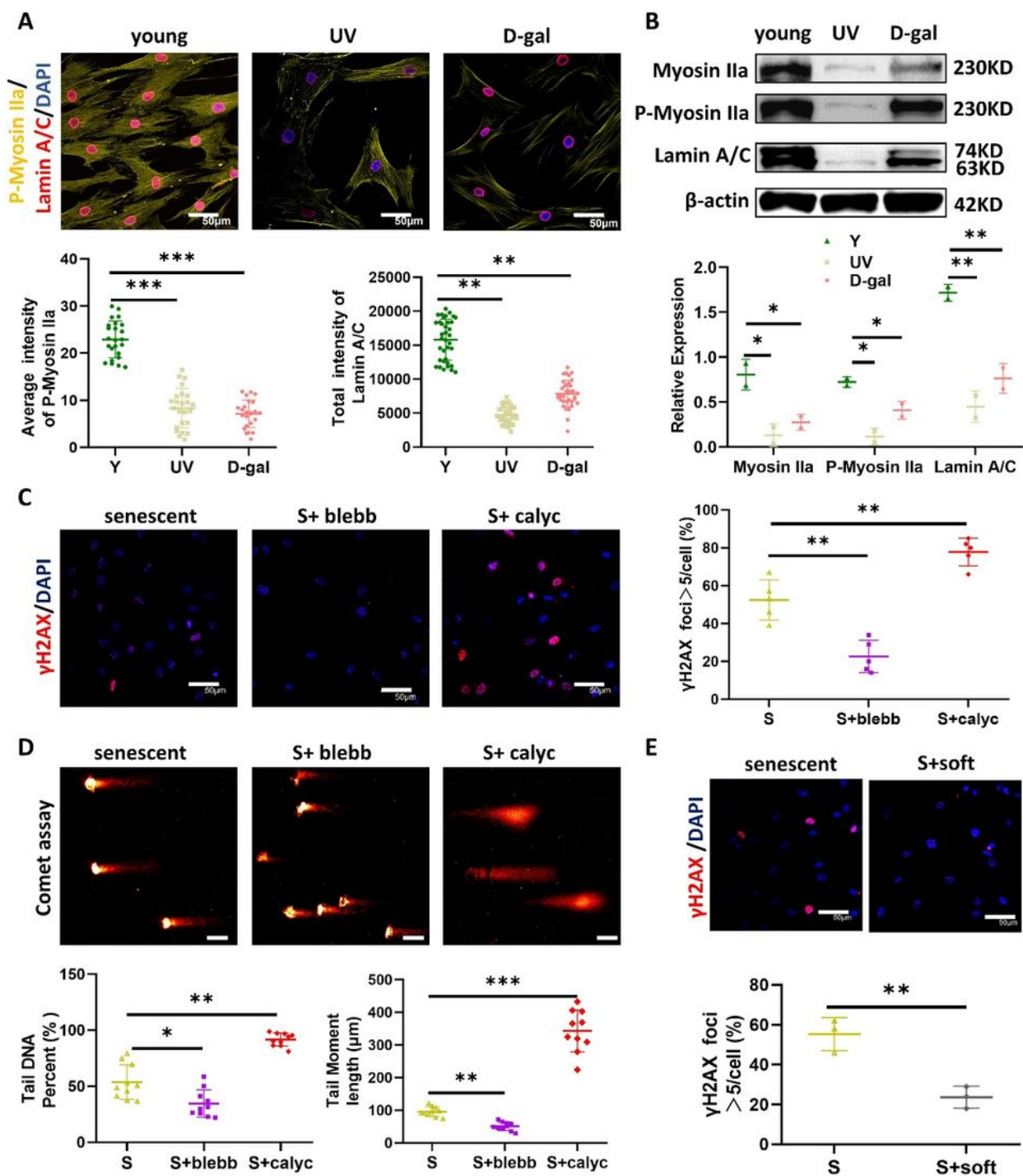


Figure 7

DNA damage crosstalk with cellular mechanotransduction.

(A) The DNA damage induced by either ultraviolet irradiation for 15 min or D-galactose for 48 h decreased the level of P-myosin IIa and Lamin A/C, as detected by immunofluorescence staining. (B) Western blot analysis of mechanotransduction markers of young BMSCs treated by ultraviolet irradiation for 15 min or D-galactose for 48 h. (C) The γ H2AX foci formation of senescent cells after exposure to blebbistatin or calyculin A for 72 h. (D) The measurement of tail DNA percent and tail moment length when senescent BMSCs were treated by blebbistatin or calyculin A for 72 h. (E) The γ H2AX foci formation is eliminated when culturing on the soft hydrogels. (Scale bar, 50 μ m)

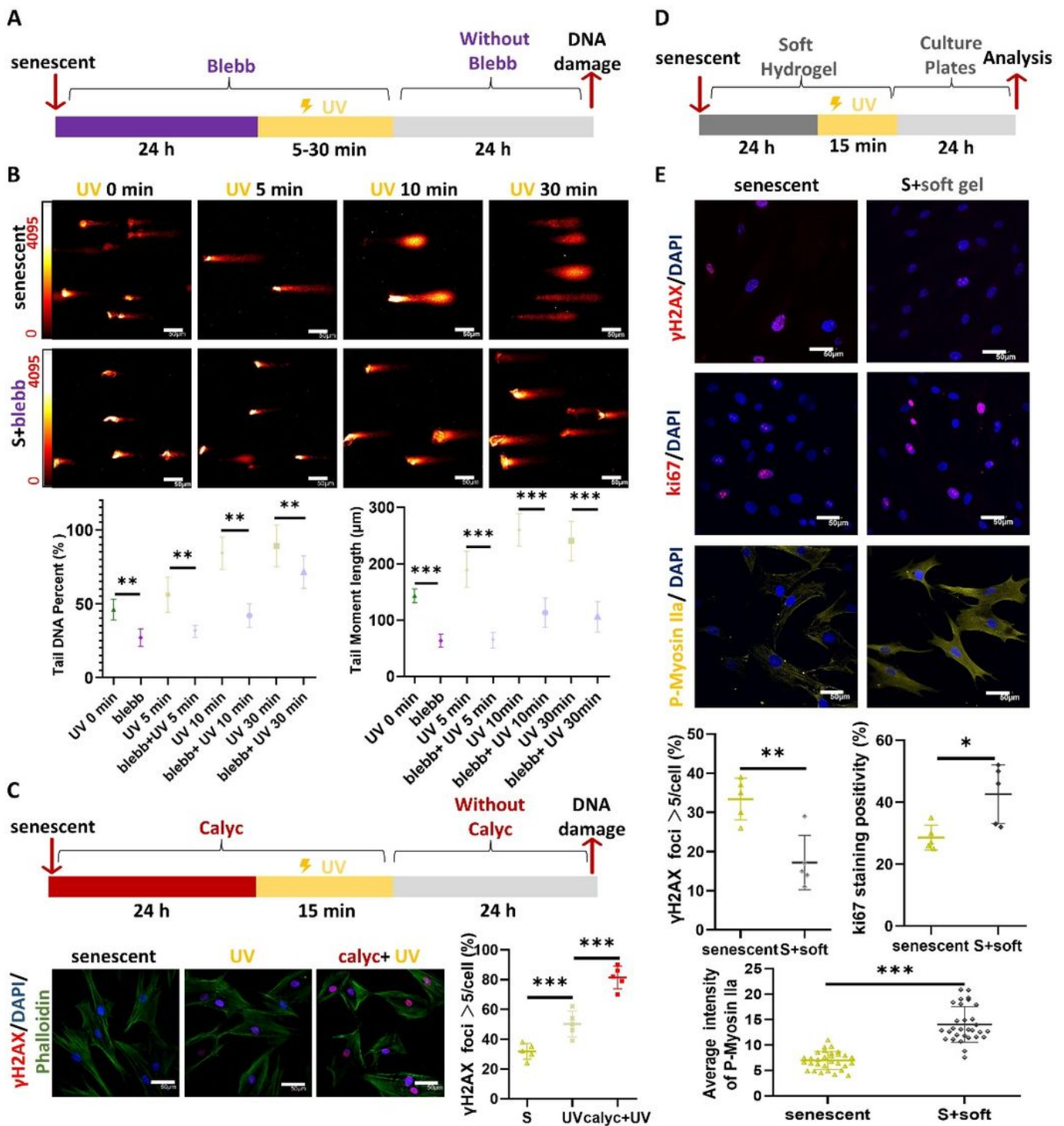


Figure 8

Mechanotransduction downregulation prevents DNA damage.

(A) Schematic of the treatment for the cells. The senescent cells were treated with blebbistatin for 24 h and then irradiated by ultraviolet for different time, followed by DNA damage analysis after 24 h culturing without drug. (B) The compromised tail DNA percent and tail moment length upon blebbistatin treatment

occurred in ultraviolet irradiated induction for different time, compared with in the absence of blebbistatin treatment. (C) The γ H2AX foci formation after being treated with calyculin A during and before ultraviolet irradiation, compared with in the absence of calyculin A. (D) Schematic of the treatment for the cells. Cells were cultured on plates or soft hydrogels for 24 h and then irradiated by ultraviolet for 15 min, followed by a series of analyses after transferring cells to culture plates. (E) The effects of soft hydrogels on γ H2AX foci formation, ki67, and P-myosin IIa levels during cells underwent ultraviolet irradiation and, the quantification of the related images. (Scale bar, 50 μ m)

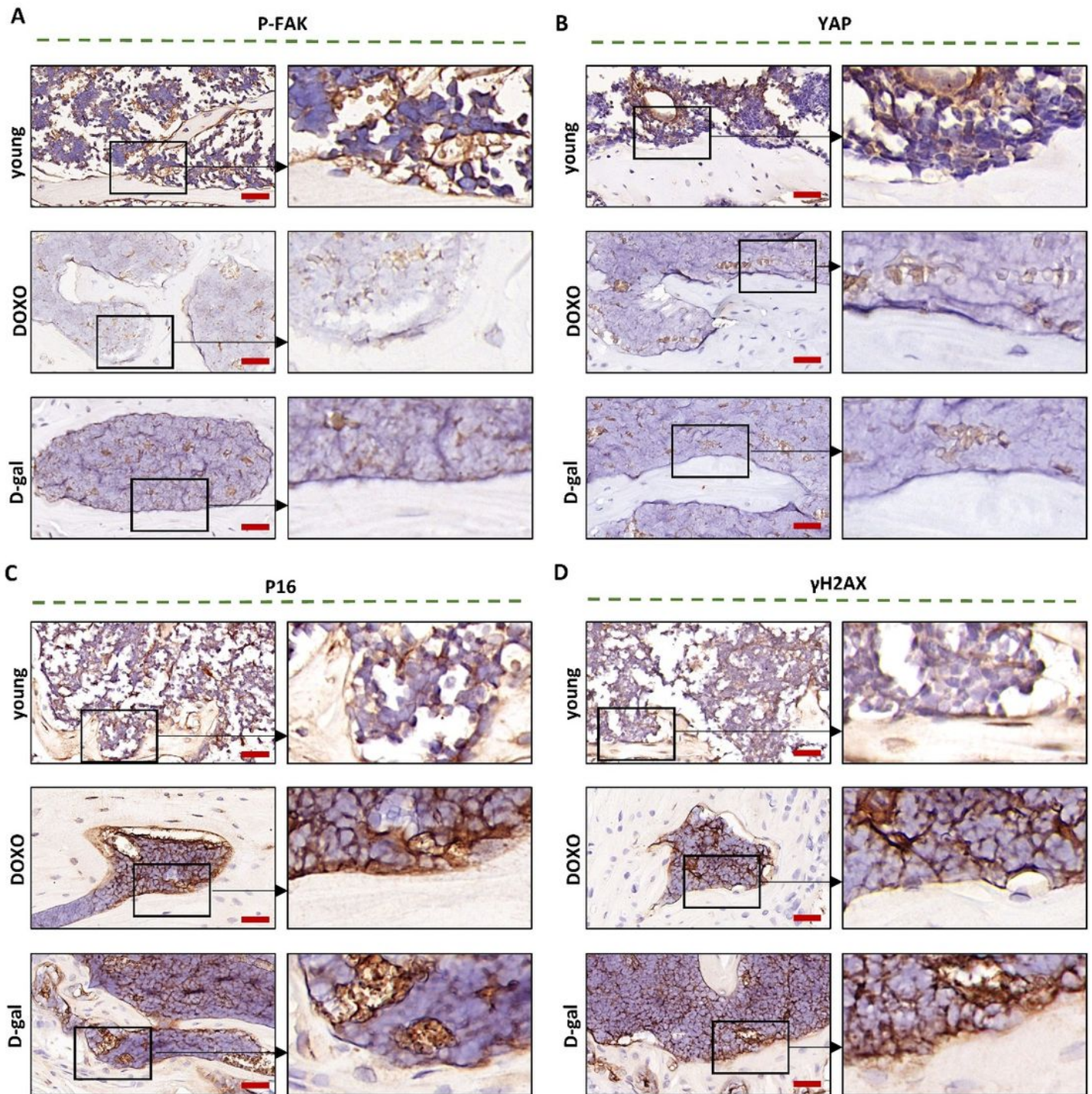


Figure 9

Bone marrow tissue shows decreased mechanotransduction activity in induced DNA damage model mice.

(A) DNA damage model mice induced by doxorubicin or D-galactose inhibited the level of P-FAK and (B) downregulated the level of YAP. (C) P16 expression and (D) the level of γ H2AX foci in different groups. (Scale bar, 100 μ m n=6)

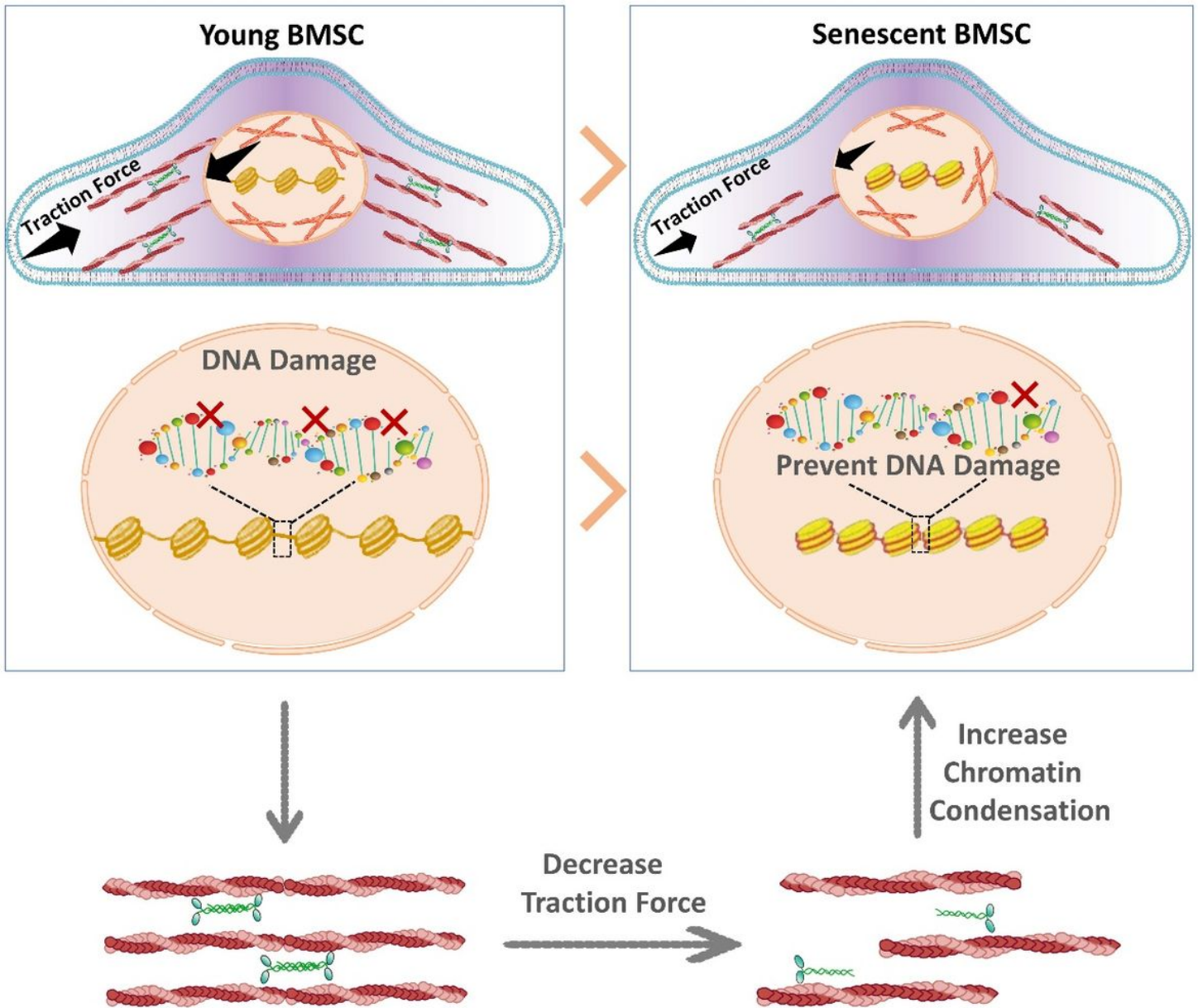


Figure 10

Working model depicting the relationships between DNA damage, cellular mechanotransduction, and cellular senescence. Upon aging, the DNA damage reduces cellular mechanotransduction activity and limits chromatin accessibility afterwards, which endows senescent BMSCs with resistance to further DNA damage.

Supplementary Files

This is a list of supplementary files associated with this preprint. Click to download.

- [Supplementaryinformation.docx](#)